Available online at www.sciencedirect.com
ScienceDirect
Journal of Photochemistry and Photobiology A: Chemistry 195 (2008) 175–182
Journal of Photochemistry and Photobiology A:Chemistry
www.elsevier.com/locate/jphotochem

Photochemical reaction of dimethylarsinous iodide in aerated methanol: A contribution to arsenic radical chemistry

Kenzo Yamanaka [a,*], Hiroshi Okimi [b], Hiroyuki Suzuki [b], Yusuke Tajima [b], Hirotaka Sonoki [b], Masahisa Osawa [b], Takashi Saito [c], Hirotomo Hase [c], Yoko Miyatake [d], Shoji Okada [e], Yoshio Miyazaki [f], Mikio Hoshino [b,**]

[a] *College of Pharmacy, Nihon University, 7-7-1 Narashinodai, Funabashi, Chiba 274-8555, Japan*
[b] *The Institute of Physical and Chemical Research (RIKEN), Wako, Saitama 351-0198, Japan*
[c] *Research Reactor Institute, Kyoto University, Kumatori, Osaka 590-0494, Japan*
[d] *Department of Mechanical Engineering, Osaka University, Toyonaka, Osaka 560-0043, Japan*
[e] *Professor Emeritus of University of Shizuoka, 2-12-7 Mariko, Suruga-ku, Shizuoka 421-0103, Japan*
[f] *Department of Chemistry, Faculty of Engineering, Toyo University, Kujirai, Kawagoe, Saitama 350-8585, Japan*

Received 26 July 2007; received in revised form 31 August 2007; accepted 2 October 2007
Available online 6 October 2007

Abstract

Continuous and laser photolysis studies of $(CH_3)_2As^{(III)}I$ were carried out in methanol solutions. The photoproduct obtained with the continuous photolysis of the aerated solutions was identified as $\{(CH_3)_2As^{(V)}(OH)_2\}^+\{(CH_3)_2As^{(V)}O(OH)\}_2][I_3^-]$ by X-ray crystallography. The laser flash photolysis of $(CH_3)_2As^{(III)}$ I in a degassed methanol gives a transient spectrum of dimethylarsine radical, $(CH_3)_2As^{(III)\bullet}$, with a broad peak centered around 560 nm. The arsinous radical, $(CH_3)_2As^{(III)\bullet}$, decays according to second order kinetics to regenerate $(CH_3)_2As^{(III)}I$. In the presence of oxygen, $(CH_3)_2As^{(III)\bullet}$ reacts with oxygen to yield the peroxy radicals, $[(CH_3)_2As^{(III)}(O_2)]^\bullet$ with the bimolecular rate constant, $2.0 \times 10^9\ M^{-1}\ s^{-1}$. The peroxy radical having weak and broad absorption in the wavelength region $\lambda > 500$ nm decays according to first order kinetics with a rate constant $5.0 \times 10^5\ s^{-1}$. It is suggested that the peroxy radical unimolecularly converts to $(CH_3)_2As^{(V)}(O)O^\bullet$, which eventually turns to the product $\{(CH_3)_2As^{(V)}(OH)_2\}^+\{(CH_3)_2As^{(V)}O(OH)\}_2][I_3^-]$.

Keywords: Laser photolysis; Dimethylarsinous iodide; Dimethylarsine radical

1. Introduction

In recent decades, much attention has been paid to the effects of inorganic arsenics on generation of human cancers [1]. Although there is limited evidence of inorganic arsenic-induced cancer in experimental animals, epidemiological surveys clearly supports the view that inorganic arsenics are the carcinogens for skin, lung and urinary bladder [2]. The effects of inorganic arsenics in mammals, however, are very complex. In 1997, arsenic trioxide was found to have anticancer activity [3–5]. The treatment of patients of acute promyelocytic leukemia, APL, with arsenic trioxide at a low dose rate possibly causes the induction of apoptosis and degradation of oncogenic promyelocytic receptor alpha fusion protein in APL cells [6–10].

Metabolic processes of inorganic arsenics have been well investigated. $As^{(III)}$ and $As^{(V)}$ taken in mammals are initially metabolized to methanearsonic acid, $CH_3As^{(V)}O(OH)_2$, and eventually dimethylarsinic acid, DMA, $(CH_3)_2As^{(V)}$ O(OH) [11–13]. The metabolite DMA partly suffers further metabolic processes before excretion in urine to yield highly toxic dimethylarsine, $(CH_3)_2As^{(III)}H$ [14,15].

Previous studies have shown that in vivo and in vitro exposure of DMA induces genetic damages: DNA strand breaks [15–18], cross-linking between DNA and nuclear proteins [19], and DNA modifications [20]. Oral administration of DMA to mice exhibits tumorigenic actions in any step of the initiation, promotion and progression [21–24]. One of the key intermediates responsible for genetic damage and tumorigenesis is suggested to

* Corresponding author. Tel.: +81 47 465 6077; fax: +81 47 465 6077.
** Corresponding author. Tel.: +81 48 461 316; fax: +81 48 461 3162.
E-mail addresses: yamanaka@pha.nihon-u.ac.jp (K. Yamanaka), hoshino@riken.jp (M. Hoshino).

1010-6030/$ – see front matter © 2007 Elsevier B.V. All rights reserved.
doi:10.1016/j.jphotochem.2007.10.002

be dimethyarsenic peroxy radical [14]. The peroxy radical is postulated to be produced by oxidation of $(CH_3)_2As^{(III)}H$ at lung and skin. In consideration for these results, International Agency for Research on Cancer (IARC) has evaluated that there is sufficient evidence for carcinogenicity of DMA in animals [2].

In this context, we have studied the chemical properties of dimethylarsenic peroxy radical formed by the reaction between the dimethylarsine radical, $(CH_3)_2As^{(III)\bullet}$ and oxygen. The dimetylarsine radical was produced by the photochemical decomposition of $(CH_3)_2As^{(III)}I$.

2. Experimental

Dimethylarsinous iodide, $(CH_3)_2As^{(III)}I$, was prepared and purified according to literature [25]. Reagent grade methanol ethanol, acetonitrile and toluene from Wako Pure Chem. Co. Ltd. were used as supplied. *N*,*N*′-tetramethyl-*p*-phenylenediamine, TMPD, from Aldrich Chem. Co. Inc. was purified by sublimation under reduced pressure. The cation radical of TMPD, $TMPD^{+\bullet}$, was obtained by oxidation of TMPD in methanol with iodine. The molar absorption coefficient of $TMPD^{+\bullet}$ in methanol was determined as $1.25 \times 10^4\ M^{-1}\ cm^{-1}$ at 610 nm by titration of TMPD with iodine.

Optical and ESR spectra were recorded on a Shimazu MPS 5000 and Jeol JES TE 200, respectively. The concentrations of oxygen in methanol solutions were determined from the gas pressure measured by a mercury and the Bunsen absorption coefficient, 0.227, of oxygen in methanol at 298 K [26].

Laser photolysis studies were carried out with a Nd-YAG laser (JK Lasers, Ltd.) equipped with second, third and fourth harmonic generators. The energy and duration of the 355 nm laser pulse are ca. 50 mJ/pulse and 20 ns, respectively. The detection systems of the transient spectra have been described elsewhere [27].

γ-Ray irradiation was performed with a 0.6 kCi ^{60}Co source at a dose rate of 25 kGy h^{-1}. Sample solutions in optical and ESR quartz cells were rapidly frozen and plunged in liquid nitrogen during the course of irradiation. The total dose absorbed by samples was ca. 12 kGy. In order to remove trapped electrons, the irradiated samples were photobleached by a 200 W tungusten lamp with a cutoff filter (λ > 450 nm) prior to optical and ESR measurements.

Continuous photolysis of $(CH_3)_2As^{(III)}I$ in aerated methanol was made by a 250 W mercury lamp (Ushio 250 D) with a cutoff filter (λ > 350 nm), which is used to avoid photolysis of solvents.

3. Results and discussion

3.1. Photochemical product from $(CH_3)_2As^{(III)}I$

An aerated methanol solution (50 cm^3) of 3.0×10^{-3} M $(CH_3)_2As^{(III)}I$ in a quartz vessel was irradiated with the mercury lamp for 6 h under stirring. The solution was exposed to air during the course of the photoreaction. The light yellowish solution gradually turned deep yellow with the irradiation time. The photoproduct is soluble in methanol. After the completion of the photoreaction, the solvent methanol in the reaction mixture was distilled off under reduced pressure. The brown viscous liquid, thus obtained, was dissolved in chloroform. The addition of ether on the surface of the chloroform solution gives deep brown plate crystals. After filtration, these crystals were subjected to the X-ray structure determination and the chemical analysis. The elemental analysis of the photoproduct is in good agreement with the molecular structure $\{(CH_3)_2As^{(V)}(OH)_2\}^+\{(CH_3)_2As^{(V)}O(OH)\}_2][I_3^-]$. Anal. Found: C; 9.13; H, 2.69; I, 47.35; As, 28.13. Calcd. for $\{(CH_3)_2As^{(V)}(OH)_2\}^+\{(CH_3)_2As^{(V)}O(OH)\}_2][I_3^-]$: C, 9.06; H, 2.79; I, 47.85; As, 28.25. The yield of the photoproduct is ca. 93%.

The continuous photolysis of $(CH_3)_2As^{(III)}I$ in aerated acetonitrile, ethanol, and toluene gives the photoproduct identical with that obtained in aerated methanol.

Crystallographic measurements of the deep brown crystals were made on a Rigaku RAXIS-IV diffractometer with Mo Kα radiation. Details of the X-ray structure analysis are summarized in Table 1. CCDC deposition codes are 635597 for $\{(CH_3)_2As^{(V)}(OH)_2\}^+\{(CH_3)_2As^{(V)}O(OH)\}_2][I_3^-]$.

Fig. 1 shows the crystal structure of the photoproduct projected along the axis determined by X-ray crystallography. The molecule is expressed as $\{(CH_3)_2As^{(V)}(OH)_2\}^+\{(CH_3)_2As^{(V)}O(OH)\}_2][I_3^-]$, in good agreement with the data of chemical analysis.

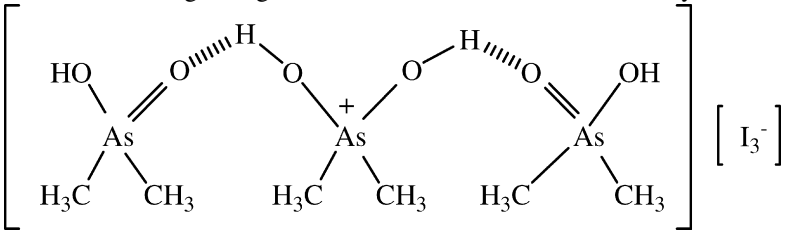

Two hydrogen bonds bridge three dimethylarsinic acid molecules. The $(CH_3)_2As^{(V)}(OH)_2\}^+$ moiety in the product has a twofold rotational axis symmetry and I_3^- ion has a center of symmetry. Fig. 2 shows the packing arrangement looking down the *b* axis. The hydrogen bonds, O(1)···O(2), $O(1)^b\cdots O(2)^b$, $O(1)^c\cdots O(2)^c$, $O(1)^d\cdots O(2)^d$, are equal in bond lengths, the value being 2.511(4) Å. These hydrogen bonds are connected along the *a* and *c* axis directions, making two dimensional network. In Table 2 are listed the selected bond lengths and angles.

Earlier X-ray crystallographic studies carried out for $[(Ph_3AsO)_2H]^+[I_3^-]$ have shown that one proton binds two $Ph_3As{=}O$ by hydrogen bonding [28]. There are two types of $[(Ph_3AsO)_2H]^+[I_3^-]$ in the unit cell. The I(1)–I(2) and I(2)–I(3)

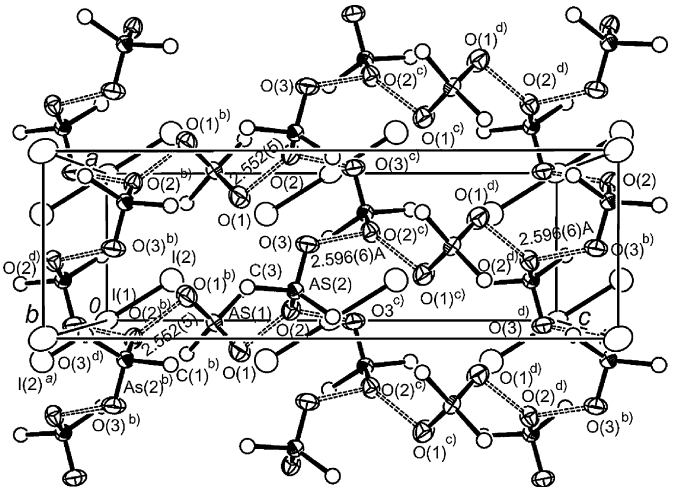

Fig. 1. The crystal structure of the photoproduct $\{(CH_3)_2As^{(V)}(OH)_2\}^+\{(CH_3)_2As^{(V)}O(OH)\}_2][I_3-]$, projected along the axis determined by X-ray crystallography.

bond distances in the $[I_3^-]$ moiety are, respectively, 2.940(2) and 2.954(1) Å for one type of $[(Ph_3AsO)_2H]^+[I_3^-]$, and those for another type of $[(Ph_3AsO)_2H]^+[I_3^-]$, 2.903(2) and 2.890(2) Å. The I–I distance of the photoproduct is in between those of the two types of $[(Ph_3AsO)_2H]^+[I_3^-]$.

The two types of $[(Ph_3AsO)_2H]^+[I_3^-]$ have the As=O bond distances different each other: one has 1.666(7)/1.685(7) Å, and another, 1.667(8)/1.674(10) Å. On the other hand, the As=O and As–O bond distances of the photoproduct are, respectively, 1.673(2) and 1.700(3)/1.706(3) Å, indicating that the As=O bond distance is very close to those of $[(Ph_3AsO)_2H]^+[I_3^-]$.

The bond angle, I(1)–I(2)–I(3), in I_3^- of the photoproduct is 180°. The configuration around each arsenic atom is almost tetrahedral as in the case of DMA, $(CH_3)_2As^{(V)}O(OH)$ [29].

As demonstrated above, the continuous photolysis of $(CH_3)_2As^{(III)}I$ in aerated methanol gives $\{(CH_3)_2As^{(V)}(OH)_2\}^+\{(CH_3)_2As^{(V)}O(OH)\}_2][I_3^-]$as the photoproduct. The brown color of the photoproduct originates from the I_3^- ion. The high yield of the photoproduct (ca. 93%) indicates that $(CH_3)_2As^{(III)}I$ in the aerate methanol solution mostly converted to $\{(CH_3)_2As^{(V)}(OH)_2\}^+\{(CH_3)_2As^{(V)}O(OH)\}_2][I_3^-]$ by the continuous photolysis. On the basis of the structure of the product, the photoreaction of $(CH_3)_2As^{(III)}I$ in aerated methanol is presumably expressed as

$$3(CH_3)_2AsI + 2H_2O + 2O_2 \xrightarrow{h\nu} [\{(CH_3)^2As^{(V)}(OH)_2\}^+ \{(CH_3)_2AsO(OH)\}_2][I_3^-] \quad (1)$$

where H_2O comes from ambient air and the solvent methanol which contains ca. 0.1% H_2O.

Table 1
X-ray data collection and processing parameters

Chemical formula	$C_6H_{22}As_3I_3O_6$
Formula weight	795.71
Space group	*Pbcn*(60)
a/Å	5.5772(3)
b/Å	21.884(2)
c/Å	17.112(2)
V/Å^3	2088.6(3)
Z	4
T/°C	−60.0
λ/Å	0.71073
D(calc)/g cm^{-3}	2.530
μ/cm^{-1}	9.221
R^a	0.0338
R_w[b]	0.0988

[a] $R = \Sigma||F_o| - |F_c||/\Sigma\,|F_o|$.

[b] $R_w = [\Sigma(w(F_o^2 - F_c^2)^2)/\Sigma w(F_o^2)^2]^{1/2}$.

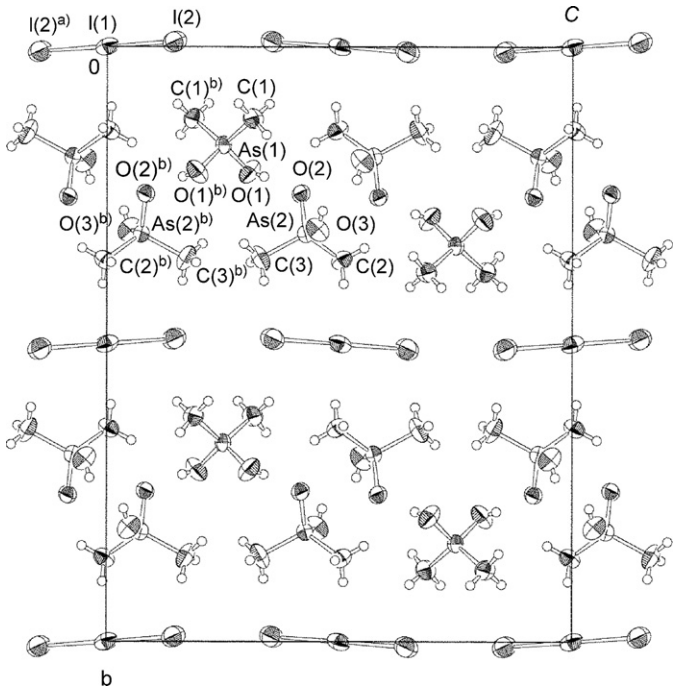

Fig. 2. The packing arrangement of the crystal looking down the *b* axis.

Table 2
Selected bond length (Å) and angles (°)

Atom	Atom	Distance	Atom	Atom	Distance
I(1)	I(2)	2.9276(3)	I(1)	I(2)[a]	2.9276(3)
As(1)	O(1)	1.700(3)	As(1)	O(1)[b]	1.700(3)
As(1)	C(1)	1.896(4)	As(1)	C(1)[b]	1.896(4)
As(2)	O(2)	1.673(2)	As(2)	O(3)	1.706(3)
As(2)	C(2)	1.898(5)	As(2)	C(3)	1.897(4)

Atom	Atom	Atom	Angle	Atom	Atom	Atom	Angle
I(2)	I(1)	I(2)[a]	180.0	O(1)	As(1)	O(1)[b]	109.7(2)
O(1)	As(1)	C(1)	110.1(2)	O(1)	As(1)	C(1)[b]	104.5(2)
O(1)[b]	As(1)	C(1)	104.5(2)	O(1)[b]	As(1)	C(1)[b]	110.2(2)
C(1)	As(1)	C(1)[b]	117.7(2)	O(2)	As(2)	O(3)	110.2(2)
O(2)	As(2)	C(2)	111.0(2)	O(2)	As(2)	C(3)	109.4(2)
O(3)	As(2)	C(2)	102.3(2)	O(3)	As(2)	C(3)	109.1(2)
C(2)	As(2)	C(3)	114.6(2)				

[a] −X, −Y, −Z.

[b] −X, Y, −Z + 1/2.

A degassed methanol solution of $(CH_3)_2As^{(III)}I$ was irradiated with the mercury lamp for 6 h. However, no photochemical decomposition of $(CH_3)_2As^{(III)}I$ was detected.

3.2. Dimethylarsine radical

The structure of the photoproduct from $(CH_3)_2As^{(III)}I$ in aerated solutions suggests that the photolysis initially undergoes the fission of the As–I bond. Earlier ESR studies have confirmed that the photolysis of dialkylarsinic halides at 77 K yields the dialkylarsine radicals by the homolytic cleavage of the As–X (X = halogen atom) bond [30,31].

The ESR spectra of dialkylarsine radicals have been well studied. However, the optical absorption spectra have not yet been reported. We have carried out γ-radiolysis of ethanol solutions of $(CH_3)_2As^{(III)}I$ at 77 K to measure the absorption and ESR spectra of dimethylarsine radical, $(CH_3)_2As^{(III)}\bullet$, at 77 K.

Fig. 3A shows the ESR spectrum observed at 77 K for an ethanol solution of 1.0×10^{-2} M $(CH_3)_2As^{(III)}I$ after γ-ray irradiation for 30 min. The spectrum exhibits four hyperfine lines due to the arsine radical. The *g*-value and the hyperfine coupling constant of the parallel component are obtained as $g_{II} = 2.002 \pm 0.001$ and $A_{II} = 242 \pm 5$ G. The perpendicular components are supposed to be hidden beneath the strong absorption of the solvent radical concomitantly produced by γ-radiolysis. The $(CH_3)_2As^{(III)}\bullet$ radical is formed by the following reactions:

$$CH_3CH_2OH \rightsquigarrow CH_3CH_2OH^{+\cdot} + e^{-\cdot} \quad (2)$$

$$CH_3CH_2OH^{+\bullet} + CH_3CH_2OH \rightarrow CH_3\dot{C}H{-}OH + CH_3CH_2{-}OH_2^{+} \quad (3)$$

$$(CH_3)_2As^{(III)}I + e^{-\bullet} \rightarrow (CH_3)As^{\bullet}\cdots I^{-} \quad (4)$$

Ionization of ethanol by γ-ray irradiation produces electrons and the ethanol cation radicals. According to Eq. (3), the cation radicals take place the ion-molecular reaction at 77 K to yield ethanol radicals and protonated ethanol molecules. The electrons produced by Eq. (2) react with $(CH_3)_2As^{(III)}I$, resulting in the formation of $(CH_3)_2As^{(III)}\bullet$ and I^- by dissociative electron attachment [32]. Because of the high viscosity of ethanol at 77 K, iodide ion, I^-, is probably located nearby $(CH_3)_2As^{(III)}\bullet$.

Fig. 3B shows the absorption spectrum observed for the γ-irradiated ethanol solution of 1.0×10^{-2} M $(CH_3)_2As^{(III)}I$ at 77 K. Since, before irradiation, the ethanol solution of $(CH_3)_2As^{(III)}I$ has no absorption at the wavelengths longer than 400 nm, the absorption band located at 560 nm is best ascribed to $(CH_3)_2As^{(III)}\bullet$. It is confirmed that the absorbance at 560 nm and the ESR signal intensity concurrently increase with an increase in the γ-irradiation time.

3.3. Laser photolysis of $(CH_3)_2As^{(III)}I$

The laser photolysis studies have been carried out for elucidation of the photochemistry of $(CH_3)_2As^{(III)}I$ in degassed and aerated methanol solutions. Fig. 4 shows the transient absorption spectra observed for the degassed methanol solution of 3.0×10^{-2} M $(CH_3)_2As^{(III)}I$ at 30 ns, 2, 10 and 100 μs after the 355 nm laser pulse. From Fig. 4, it is concluded that the transient spectrum at 30 ns is composed of two absorption bands: one is located around 560 nm and the other, $\lambda < 420$ nm. The

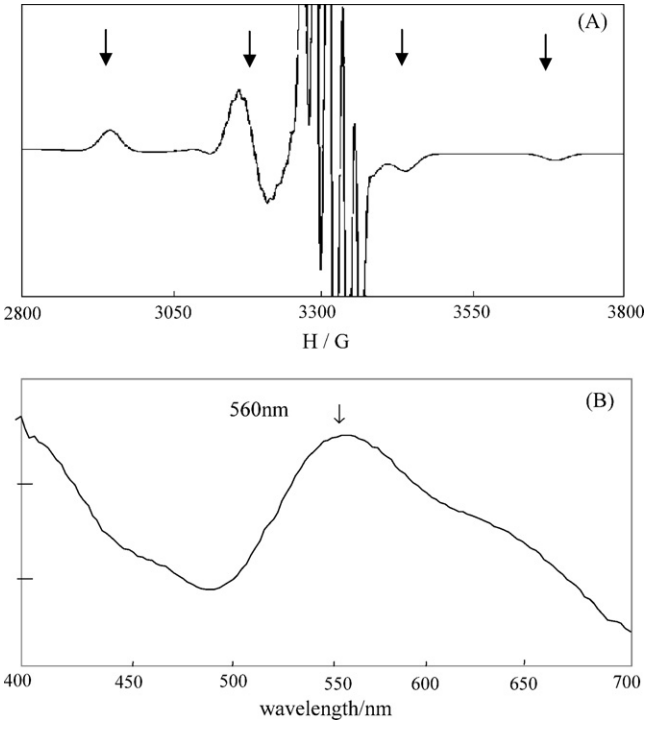

Fig. 3. The ESR (A) and the optical absorption (B) spectra observed for an ethanol solution of 1.0×10^{-2} M $(CH_3)_2As^{(III)}I$ after γ-ray irradiation for 30 min at 77 K. The strong central lines in (A) are due to the solvent radicals produced by γ-ray irradiation at 77 K.

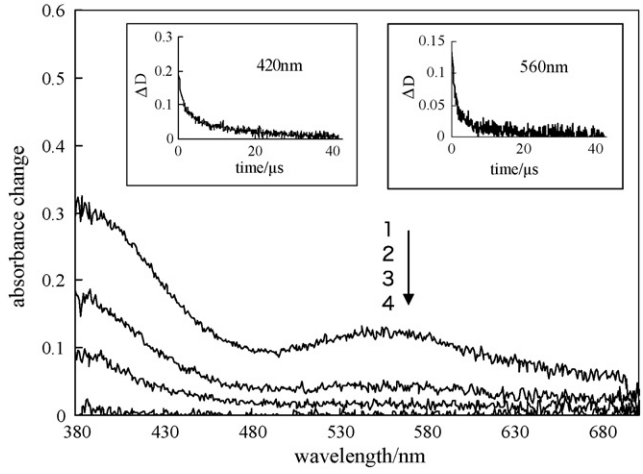

Fig. 4. The transient absorption spectra observed for a degassed methanol solution of 1.0×10^{-2} M $(CH_3)_2As^{(III)}I$ after the 355 nm laser pulse: (1) 30 ns, (2) 2 μs, (3) 10 μs and (4) 100 μs. The insets are the oscilloscope traces monitored at 420 and 560 nm.

long wavelength band around 560 nm is very similar to that of $(CH_3)_2As^{(III)\bullet}$ produced by γ-radiolysis of $(CH_3)_2As^{(III)}I$ in ethanol at 77 K. The time profiles of the absorbance change observed at 420 and 560 nm are shown in the insets of Fig. 4. The 560-nm band decays according to second order kinetics, and disappears within 10 μs after the pulse: the value of the apparent bimolecular rate constant, $k_{bi}/\varepsilon_{560\,nm}$, measured at 560 nm is obtained as $k_{bi}/\varepsilon_{560\,nm} = 1.6 \times 10^7\ cm\ s^{-1}$. We consider that the transient having the absorption band around 560 nm is ascribed to $(CH_3)_2As^{(III)\bullet}$. The photochemical formation of $(CH_3)_2As^{(III)\bullet}$ from $(CH_3)_2As^{(III)}I$ in degassed methanol is described as

$$(CH_3)_2As^{(III)}I \xrightarrow{h\nu} (CH_3)_2As^{(III)\bullet} + I \quad (5)$$

$$(CH_3)_2As^{(III)\bullet} + I \rightarrow (CH_3)_2As^{(III)}I \quad (6)$$

Dimethylarsine radicals are produced by homolytic cleavage of the As–I bond in $(CH_3)_2As^{(III)}I$. Here we consider that the major pathway returning to the parent molecule is the recombination reaction of $(CH_3)_2As^{(III)\bullet}$ and I.

Dimethylarsine radicals produced by homolytic cleavage of the As–I bond in $(CH_3)_2As^{(III)}I$ recombine with iodine atoms, returning to the parent molecule as represented in Eq. (6).

The decay profile of the absorbance at 420 nm is found to be different from that at 560 nm. It seems that the decay measured at 420 nm shown in the inset of Fig. 4 is composed of two species: the faster and the slower decay component. Although the slower decay component is not identified, the faster decay component is possibly ascribed to $(CH_3)_2As^{(III)\bullet}$. On the assumption that the faster and slower components decay according to second order kinetics, the absorbance $D(t)$ at 420 nm is represented as

$$D(t) = D(t)_f + D(t)_s = (k_{f/\varepsilon_{420}}t + \alpha)^{-1} + (k_{f/\varepsilon_{420}}t + \beta)^{-1} \quad (7)$$

Here, $D(t)_f$ and $D(t)_s$ are the absorbances of the faster and the slower decay components at time t after the laser pulse, respectively. k_f/ε_{420} and k_s/ε_{420} are, respectively, the apparent bimolecular rate constants of the faster and the slower decay component, and $\alpha = [D(0)_f]^{-1}$ and $\beta = [D(0)_s]^{-1}$.

The values of k_f/ε_{420} and k_s/ε_{420} were determined as $k_f/\varepsilon_{420} = 1.7 \times 10^7\ cm\ s^{-1}$ and $k_s/\varepsilon_{420} = 8.0 \times 10^4\ cm\ s^{-1}$ from the curve fitting of the decay profile of the absorbance at 420 nm with the use of Eq. (7) and the least squares fitting program. The former value, $k_f/\varepsilon_{420} = 1.7 \times 10^7\ cm\ s^{-1}$, is in good accord with k_{bi}/ε_{560} obtained from the decay analysis at 560 nm, indicating that ε_{420} is close to ε_{560}.

The spectrum of the faster decay component $(CH_3)_2As^{(III)\bullet}$ can be obtained by subtracting the transient spectrum measured at 10 μs from that at 30 ns. Fig. 5 shows the difference spectrum thus obtained. The spectrum is moderately in good agreement with that of $(CH_3)_2As^{(III)\bullet}$ shown in Fig. 3B. From Fig. 5, it is found that the molar absorption coefficient of $(CH_3)_2As^{(III)\bullet}$ at 420 nm is almost identical with that at 560 nm, in agreement with results of the decay analysis of $(CH_3)_2As^{(III)\bullet}$ mentioned above.

Earlier ESR studies have shown that low temperature photolysis of $(CH_3)_2As^{(III)}I$ gives the dimethylarsine radical, $(CH_3)_2As^{(III)\bullet}$, and the cation radical, $\{(CH_3)_2As^{(III)}I\}^{+\bullet}$, The

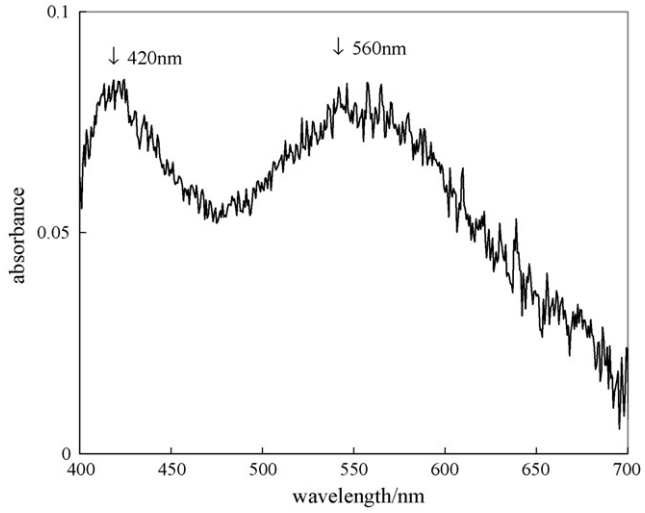

Fig. 5. The difference spectrum obtained by subtracting the transient spectrum observed at 10 μs from that at 30 ns.

unidentified slower decay component with an absorption band around 400 nm observed by the laser photolysis could be due to the cation radical, $\{(CH_3)_2As^{(III)}I\}^{+\bullet}$, produced by photoionization of $(CH_3)_2As^{(III)}I$ in methanol.

According to Eq. (5), photolysis of $(CH_3)_2As^{(III)}I$ results in the formation of atomic iodine, I. We have carried out the laser photolysis of molecular iodine, I_2, in toluene to measure the absorption spectrum of I: photolysis of I_2 gives I [33]. The 355 nm laser photolysis of I_2 in toluene affords a weak and broad absorption band around 500 nm, which disappears according to second order kinetics. Since the transient spectra in Fig. 4 does not exhibit the absorption band ascribable to I, we assume that the weak absorption band of I liberated from Eq. (2) is hidden beneath the transient spectra of $(CH_3)_2As^{(III)\bullet}$ taken after the laser pulse.

Laser photolysis of $(CH_3)_2As^{(III)}I$ in aerated methanol was carried out with an aim to understand the reaction mechanism for the formation of the photoproduct, $\{(CH_3)_2As^{(V)}(OH)_2\}^+\{(CH_3)_2As^{(V)}O(OH)\}_2][I_3^-]$, isolated by the continuous photlysis. Fig. 6 shows the transient absorption spectra observed for an aerated methanol solution of 1.0×10^{-2} M $(CH_3)_2As^{(III)}I$ after the 355 nm laser pulse. The transient spectrum detected at 30 ns after the pulse is in good agreement with that observed in the degassed methanol solution. From this result, we conclude that the initial photochemical events of $(CH_3)_2As^{(III)}I$ in an aerated solution are the same as those in a degassed system.

The insets in Fig. 6 show the decay profiles of the 560 and 700 nm absorbances. With an increase in time, the absorbance at 560 nm disappears within 4 μs after the pulse. The 700 nm band exhibits the biphasic decay: the faster decay observed within 2 μs and the slower decay later than 2 μs after the pulse. We consider that the decay of the 560 and 700 nm band is explained by assuming that $(CH_3)_2As^{(III)\bullet}$ produced by photolysis of $(CH_3)_2As^{(III)}I$ in aerated methanol reacts with oxygen to yield the intermediate, $(CH_3)_2As^{(III)}(O_2)^\bullet$ which undergoes further decay. The decay of the 560 nm absorbance is principally

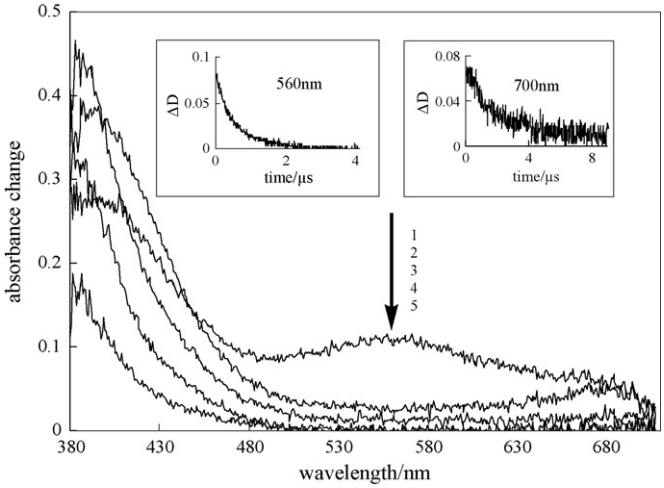

Fig. 6. The transient absorption spectra observed for an aerated methanol solution of 1.0×10^{-2} M $(CH_3)_2As^{(III)}I$ after the 355 nm laser pulse; (1) 30 ns, (2), 500 ns (3), 10 μs (4), 50 μs and (5) 500 μs. The insets are the oscilloscope traces monitored at 560 and 700 nm.

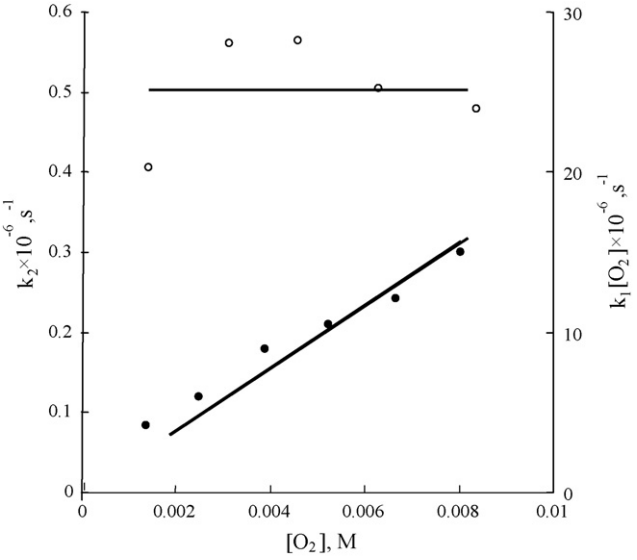

Fig. 7. The plots of $k_1[O_2]$ and k_2 against $[O_2]$ (see text).

ascribed to $(CH_3)_2As^{(III)\bullet}$. However, the absorbance change at 700 nm is due to the sum of the decay of $(CH_3)_2As^{(III)\bullet}$ and the formation and decay of $(CH_3)_2As^{(III)}$ $(O_2)^\bullet$ concomitantly produced by the reaction of $(CH_3)_2As^{(III)\bullet}$ and O_2. The transient spectrum observed at ca. 2 μs after the decay of $(CH_3)_2As^{(III)\bullet}$ is assumed to be ascribed to the peroxy radical, $(CH_3)_2As^{(III)}$ $(O_2)^\bullet$, which is supposed to be intramolecularly transformed to $(CH_3)_2As^{(V)}$ $(O)O^\bullet$.

$$(CH_3)_2As^{(III)\bullet} + O_2 \xrightarrow{k_1[O_2]} (CH_3)_2As^{(III)}(O_2)^\bullet \quad (8)$$

$$(CH_3)_2As^{(III)} + (O_2)^\bullet \xrightarrow{k_2} (CH_3)_2As^{(V)}(O)O^\bullet \quad (9)$$

Thus, the faster and the slower decay of the 560 and 700 nm bands are, respectively, ascribed to Eqs. (7′) and (8). With the use of Eqs. (8) and (9), the rate equations for $(CH_3)_2As^{(III)}$ and $(CH_3)_2As^{(III)}$ $(O_2)^\bullet$ are formulated as

$$\frac{-dA}{dt} = k_1[O_2]A \quad (10)$$

$$\frac{dB}{dt} = k_1[O_2]A - k_2B \quad (11)$$

where A and B stand for the concentrations of $(CH_3)_2As^{(III)\bullet}$ and $(CH_3)_2As^{(III)}$ $(O_2)^\bullet$, respectively. Eqs. (10) and (11) are transformed to

$$sA = A_0 \ \exp(-k_1[O_2]t) \quad (12)$$

$$B = \frac{k_1[O_2]A_0}{k_2 - k_1[O_2]}\{\exp(-k_1[O_2]t) - \exp(-k_2t)\} \quad (13)$$

Here A_0 is the concentration of $(CH_3)_2As^{(III)\bullet}$ at $t = 0$.

Thus, the absorbance of the transient spectrum at λ, $D(\lambda)$ is written as

$$D(\lambda) = \varepsilon_A(\lambda)A + \varepsilon_B(\lambda)B = \varepsilon_A(\lambda)A_0 \ \exp(-k_1[O_2]t) + \frac{k_1[O_2]\varepsilon_B(\lambda)A_0}{k_2 - k_1[O_2]}\{\exp(-k_1[O_2]t) - \exp(-k_2t)\} \quad (14)$$

where $\varepsilon_A(\lambda)$ and $\varepsilon_B(\lambda)$ are the molar absorption coefficients of $(CH_3)_2As^{(III)\bullet}$ and $(CH_3)_2As^{(III)}$ $(O_2)^\bullet$ at the wavelength λ, respectively.

The decay analysis of $(CH_3)_2As^{(III)\bullet}$ monitored at 560 nm was carried out by using Eq. (14) with $\varepsilon_{\equiv}(560\,nm) = 0$ and a least squares fitting program. The rate constants, $k_1[O_2]$, were determined by changing the concentration of oxygen in methanol. As shown in Fig. 7, the plot of $k_1[O_2]$ vs. $[O_2]$ gives a straight line. The slope of the line affords $k_1 = 2.0(\pm 0.2) \times 10^9\ M^{-1}\ s^{-1}$. The k_2 value is obtained from the decay analysis of the 700 nm band with the use of Eq. (14), the k_1 value obtained above, and the least squares fitting program. The rate constant was determined as $k_2 = 5.0\ (\pm 1.0) \times 10^5\ s^{-1}$. As represented in Fig. 7, this value is independent of $[O_2]$ in the concentration range $4.2 \times 10^{-4}\ M < [O_2] < 8.4 \times 10^{-3}\ M$.

The time profile of the absorbance at 420 nm was much complicated: both the rise and the decay were observed after the laser pulse. Since the rise time in the time profile of the 420 nm absorbance is close to the decay time of the 560 nm band, the rise of the absorbance at 420 nm is assumed to be, at least in part, due to the formation of $(CH_3)_2As^{(III)}$ $(O_2)^\bullet$ by oxidation of $(CH_3)_2As^{(III)\bullet}$. The decay at the 420 nm absorbance was found to be approximately expressed as a sum of the two exponential functions of time: the faster decay component has the rate constant of $3.0 \times 10^5\ s^{-1}$, and the slower one, $1.2 \times 10^4\ s^{-1}$, respectively. The former value is moderately close to the decay rate constant of $(CH_3)_2As^{(III)}$ $(O_2)^\bullet$ as obtained from the decay analysis of the 520 nm band.

As represented in Eq. (1), three $(CH_3)_2As^{(III)}I$, two O_2, and two H_2O molecules are necessary to yield the final photoproduct. The initial event, however, is considered to be the photodissociation of the As–I bond in $(CH_3)_2As^{(III)}I$ followed by the oxidation of $(CH_3)_2As^{(III)\bullet}$.

The photoproduct from $(CH_3)_2As^{(III)}I$ in aerated methanol consists of three dimethylarsinous acid and one HI_3. The laser photolysis studies indicate that the transients observed

after the laser pulse are $(CH_3)_2As^{(III)\bullet}$ and the unidentified intermediate, which is tentatively assumed to be $\{(CH_3)_2As^{(III)}I\}^{+\bullet}$. Taking account of the fact that the yield of the photoproduct in aerated methanol is ca. 93%, we consider that, although not quantitative, both $(CH_3)_2As^{(III)\bullet}$ and the unidentified intermediate are oxidized by oxygen, eventually leading to the formation of the photoproduct, $\{(CH_3)_2As^{(V)}(OH)_2\}^+\{(CH_3)_2As^{(V)}O(OH)\}_2][I_3^-]$.

The kinetic analysis studies of the transient spectra of $(CH_3)_2As^{(III)}I$ in aerated methanol indicate that the reaction of $(CH_3)_2As^{(III)\bullet}$ and oxygen gives the peroxy radical, $(CH_3)_2As^{(III)}(O_2)^\bullet$, which undergoes intramolecular transformation to yield $(CH_3)_2As^{(V)}(O)O^\bullet$. We suppose that $(CH_3)_2As^{(III)}$ $(O_2)^\bullet$ and $(CH_3)_2As^{(V)}(O)O^\bullet$ play a key role in cancer generation by arsinous compounds in vivo. In order to examine whether or not both $(CH_3)_2As^{(III)}(O_2)^\bullet$ and $(CH_3)_2As^{(V)}(O)O^\bullet$ are the oxidizing reagents [34], the laser photolysis studies of $(CH_3)_2As^{(III)}I$ in an aerated methanol solutions containing *N*,*N*′-tetramethyl-*p*- phenylenediamine, TMPD, were carried out. It is known that one-electron oxidation of TMPD results in the formation of the blue cation radical, $TMPD^{+\bullet}$ [35]. However, we could not detect $TMPD^{+\bullet}$ after the laser pulse, suggesting that the photochemical oxidation products from $(CH_3)_2$ $As^{(III)}I$ in aerated methanol are unable to oxidize TMPD.

During the course of this study, we found that blue $TMPD^{+\bullet}$ is readily bleached by irradiation of $(CH_3)_2As^{(III)}I$ in aerated methanol. This finding suggests that the transient oxidation product from$(CH_3)_2As^{(III)}I$ reacts with $TMPD^{+\bullet}$, leading to the decomposition of $TMPD^{+\bullet}$. A possible candidate of the transient oxidation product is the superoxide anion radical, which can reduce $TMPD^{+\bullet}$ to TMPD.

$$TMPD^{+\bullet} + O_2^{-\bullet} \rightarrow TMPD + O_2 \tag{15}$$

However, regeneration of TMPD was not found in the irradiated solution, indicating that the super oxide anion radical is not responsible for the bleaching of $TMPD^{+\bullet}$

We assume that the peroxy radical, $(CH_3)_2As^{(III)}(O_2)^\bullet$, bleaches $TMPD^{+\bullet}$:

$$TMFD^{+\bullet} + (CH_3)_2As^{(III)}O_2^\bullet \xrightarrow{k_c} \text{bleached adduct} \tag{16}$$

From Eqs. (9) and (16), the rate equations for $(CH_3)_2As^{(III)}O_2^\bullet$ and $TMPD^{+\bullet}$ are represented as

$$\frac{-d[(CH_3)_2As^{(III)}O_2^\bullet]}{dt} = k_c[TMPD^{+\bullet}][(CH_3)_2As^{(III)}O_2^\bullet] + k_2[(CH_3)_2As^{(III)}O_2^\bullet] \tag{17}$$

$$\frac{-d[TMPD^{+\bullet}]}{dt} = k_c[TMPD^{+\bullet}][(CH_3)_2As^{(III)}O_2TMPD^{+\bullet}] \tag{18}$$

When $[TMPD^{+\bullet}] \gg [(CH_3)_2As^{(III)}O_2^\bullet]$, the concentration of $TMPD^{+\bullet}$ is approximately invariable during the bleaching of $TMPD^{+\bullet}$ by $(CH_3)_2As^{(III)}O_2^\bullet$. Thus, the following equation is obtained.

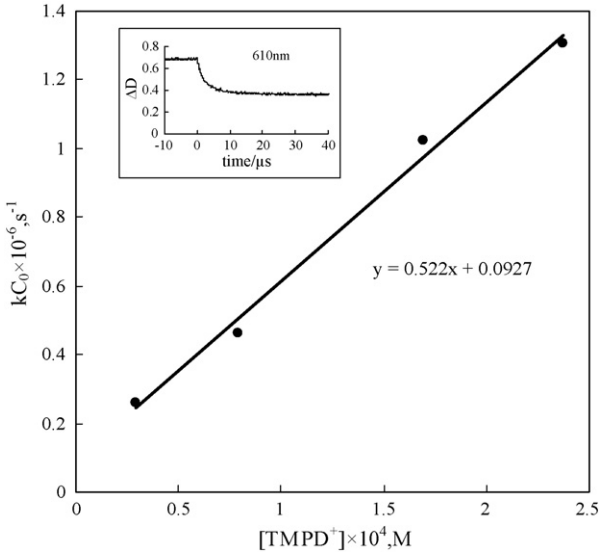

Fig. 8. The plot of k_d against the concentration of $TMPD^{+\bullet}$. The inset is the oscilloscope trace observed at 610 nm.

$$\Delta D = \Delta D_0\{1 - \exp(-k_{obsd}t)\} \tag{19}$$

where ΔD and ΔD_0 are the absorbance changes at time t and at an *infinite* time, respectively, and k_{obsd} is expressed as

$$k_{obsd} = k_d[TMPD^{+\bullet}] + k_2. \tag{20}$$

In the present study, the concentrations of $TMPD^{+\bullet}$ used are $1.0 \times 10^{-4}\,M < [TMPD^{+\bullet}] < 6.2 \times 10^{-4}\,M$. It was found that, when $[TMPD^{+\bullet}] > 1.0 \times 10^{-4}\,M$, the amount of the photobleached $TMPD^{+\bullet}$ after the pulse is less than 15% of the initial concentration of $TMPD^{+\bullet}$. The inset in Fig. 7 shows the time profile for the bleaching of $TMPD^{+\bullet}$ monitored at 610 nm. The decay of the 610-nm absorbance was well represented by Eq. (18): the rate constants, k_{obsd}, are determined from Eq. (19) and the least squares fitting method.

Fig. 8 shows the plot of the rate constant, k_{obsd}, represented as a function of the initial concentration of $TMPD^{+\bullet}$. The plot gives a straight line.

The slope of the line gives the bimolecular rate constant, $k_d = 2.7 \times 10^9\,M^{-1}\,s^{-1}$, and the intercept, $k_2 = 5.6 \times 10^5\,s^{-1}$. The value of k_2 is very close to that previously determined from the decay analysis of the 700 nm band of the transients detected by the laser photolysis of $(CH_3)_2As^{(III)}I$ in aerated methanol. On the basis of these results, it is suggested that the transient oxidation product responsible for bleaching of $TMPD^{+\bullet}$ is ascribed to $(CH_3)_2As^{(III)}(O_2)^\bullet$.

We tried to separate and identify the decomposition products yielded by photolysis of $(CH_3)_2As^{(III)}I$ in aerated methanol containing $TMPD^{+\bullet}$. Unfortunately, the products were the viscous polymers and the identification cannot be made. Presumably, the addition product formed between $(CH_3)_2As^{(III)}(O_2)^\bullet$ and $TMPD^{+\bullet}$ suffers further oxidation in aerated methanol, leading to the bleaching of $TMPD^{+\bullet}$.

4. Conclusions

Continuous and laser photolysis studies of $(CH_3)_2As^{(III)}I$ revealed that the As–I bond in $(CH_3)_2As^{(III)}I$ is photodissociated to yield the $(CH_3)_2As^{(III)\bullet}$ radical. In aerated methanol, the $(CH_3)_2As^{(III)\bullet}$ radical readily reacts with oxygen with the rate constant, $k_1 = 2.0\ (\pm 0.2) \times 10^9\ M^{-1}\ S^{-1}$, resulting in the formation of the peroxy radical, $(CH_3)_2As^{(III)}(O_2)^\bullet$. The peroxy radical is unimolecularly transformed to $(CH_3)_2As^{(V)}(O)O^\bullet$ radical with the first order rate constant, $k_2 = 5.0\ (\pm 1.0) \times 10^5\ s^{-1}$. The present result shows that (1) both $(CH_3)_2As^{(III)}(O_2)^\bullet$ and $(CH_3)_2As^{(V)}(O)O^\bullet$ in methanol are unable to oxidize TMPD and (2) $(CH_3)_2As^{(III)}(O_2)^\bullet$ has a high reactivity toward $TMPD^{+\bullet}$, resulting in the bleaching of $TMPD^{+\bullet}$.

Acknowledgements

The present work was supported in part by a Grant-in-Aid for Scientific Research (C) (No. 17590110) from the Ministry of Education, Culture, Sports, Science, and Technology of Japan, and "Academic Frontier" Project for Private Universities: matching fund subsidy from MEXT (the Ministry of Education, Culture, Sports, Science, and Technology) 2002–2006.

References

[1] IARC, IARC monographs on the evaluation of carcinogenic risk of chemicals to humans Some Metals and Metallic Compounds, vol. 23, IARC, Lyon, 1980, pp. 39–141.
[2] IARC, IARC monographs on the evaluation of carcinogenic risks to humans Some Drinking-Water Disinfectants and Contaminants, Including Arsenic, vol. 84, IARC, Lyon, 2004, pp. 41–267.
[3] Z.X. Shen, G.Q. Chen, J.H. Ni, X.S. Li, S.M. Xiong, Q.Y. Qiu, J. Zhu, W. Tang, G.L. Sun, K.Q. Yang, Y. Chen, L. Zhou, Z.W. Fang, Y.T. Wang, J. Ma, P. Zhang, T.D. Thang, S.J. Chen, Z. Chen, Z.Y. Wang, Blood 89 (1997) 3354–3360.
[4] S.L. Soignet, P. Maslak, Z.G. Wang, S. Jhanwar, E. Calleja, L.J. Dardashti, D. Corso, A. DeBlasio, J. Gabrilove, D.A. Scheinberg, P.P. Pandorfi, R.P. Warrell Jr., Engl. J. Med. 339 (1998) 1341–1348.
[5] S.K. Bergstrom, E. Gillan, J.J. Quinn, A.J. Altman, J. Pedatr. Hematol. Oncol. 20 (1998) 545–547.
[6] G.Q. Chen, X.J. Zhu, G. Shi, J.H. Ni, H.J. Zhong, G.Y. Shi, X.L. Jin, W. Tang, X.S. Li, S.M. Xong, Z.X. Shen, G.L. Sun, J. Ma, P. Zhang, T.D. Zhang, C. Gazin, T. Naoe, S.J. Chen, Z.Y. Wang, Z. Chen, Blood 88 (1996) 1052–1061.
[7] Z.G. Wang, R. Rivi, L. Delva, A. Konig, D.A. Scheinberg, C. Gambacorti-Passerini, J.L. Gabrilove, R.P. Warrell Jr., P.P. Pandorfi, Blood 92 (1998) 1497–1504.
[8] M. Gianni, M.H. Koken, M.K. Chelbi-Alix, G. Benoit, M. Lannotte, Z. Chen, H. de The, Blood 91 (1998) 4300–4310.
[9] Z. Chen, Z.Y. Wang, S. Chen, J. Pharmacol. Ther. 76 (1997) 141–149.
[10] W. Shao, M. Fanelli, F.F. Ferrara, R. Riccioni, A. Rosenauer, K. Davison, W.W. Lamp, S. Waxman, P.G. Pelicci, F. Lo Coco, G. Avvisati, U. Testa, C. Peschule, C. Gambacorti-Passerini, C. Nervi, W.H. Miller Jr., J. Natl. Cancer Inst. 90 (1998) 124–133.
[11] M. Vahter, Environ. Res. 25 (1981) 286–293.
[12] M. Vahter, E. Marafante, Chem. Biol. Interactions 47 (1983) 29–44.
[13] M. Vahter, E. Marafante, Toxicol. Lett. 37 (1987) 41–46.
[14] K. Yamanaka, M. Hoshino, M. Okamoto, R. Sawamura, A. Hasegawa, S. Okada, Biochem. Biophys. Res. Commun. 168 (1990) 58–64.
[15] K. Yamanaka, S. Okada, Environ. Health Persp. 102 (suppl. 3) (1994) 37–40.
[16] M. Tezuka, K. Hanioka, K. Yamanaka, S. Okada, Biochem. Biophys. Res. Commun. 191 (1993) 1178–1183.
[17] J.L. Brown, K.T. Kitchin, M. George, Tetratogen. Carcinogen. Mutagen. 17 (1997) 71–84.
[18] S. Ahmad, W.L. Anderson, K.T. Kitchin, Cancer Lett. 139 (1999) 129–135.
[19] K. Yamanaka, M. Tezuka, K. Kato, A. Hasegawa, S. Okada, Biochem. Biophys. Res. Commun. 191 (1993) 1184–1191.
[20] K. Yamanaka, H. Hayashi, M. Tachikawa, K. Kato, A. Hasegawa, N. Oku, S. Okada, Mutat. Res. 394 (1997) 95–101.
[21] K. Yamanaka, K. Ohtsubo, A. Hasegawa, H. Hayashi, H. Ohji, M. Kanisawa, S. Okada, Carcinogenesis 17 (1996) 767–770.
[22] H. Hayashi, M. Kanisawa, K. Yamanaka, T. Ito, N. Udaka, H. Ohji, K. Okudela, S. Okada, H. Kitamura, Cancer Lett. 125 (1998) 83–88.
[23] S. Yamamoto, Y. Konishi, T. Matsuda, T. Murai, M. Shibata, I. Matsui-Yuasa, S. Ohtani, K. Kuroda, G. Endo, S. Fukushima, Cancer Res. 55 (1995) 1271–1276.
[24] H. Wanibuchi, S. Yamamoto, H. Cohen, K. Yoshida, G. Endo, T. Hori, S. Fukushima, Carcinogenesis 17 (1997) 2435–2439.
[25] E. Roberts, E. Turner, F.W. Bury, J. Chem. Soc. (1926) 1443–1447.
[26] C.L. Young (Ed.), IUPAC Solubility Data Series, 8, Pergamon Press, New York, 1985.
[27] M. Hoshino, H. Sonoki, Y. Miyazaki, Y. Iimura, K. Yamamoto, Inorg. Chem. 39 (2000) 4850–4857.
[28] B. Beagley, O. EI-Sayrafi, G.A. Gott, D.G. Kelly, C.A. McAuliffe, A.G. Mackie, P.P. MacRory, R.G. Pritchard, J. Chem. Soc. Dalton Trans. (1988) 1095–1097.
[29] J. Trotter, T. Zobel, J. Chem. Soc. (1965) 4466–4471.
[30] A.R. Lyons, M.C.R. Symons, J. Am. Chem. Soc. 95 (1973) 3483–3485.
[31] J.R. Preer, F.-D. Tsay, H.B. Gray, J. Am. Chem. Soc. 94 (1972) 1875–1880.
[32] W.H. Hamill, in: E.T. Kaiser, L. Kevan (Eds.), Radical Ions, Wiley, New York, 1968, p. 321.
[33] L. Meadows, R.M. Noyes, J. Am. Chem. Soc. 82 (1960) 1872–1876.
[34] M. Hoshino, K. Kagata, H. Seki, H. Seto, J. Am. Chem. Soc. 118 (1996) 2160–2665.
[35] J.T. Richard, J.K. Thomas, Trans. Far. Soc. 66 (1970) 621–632.